



ELSEVIER

Journal of Electroanalytical Chemistry 520 (2002) 71–78

Journal of
Electroanalytical
Chemistry

www.elsevier.com/locate/jelechem

Direct electrochemical reduction of hemin in imidazolium-based ionic liquids

David L. Compton*, Joseph A. Laszlo

United States Department of Agriculture¹, Agricultural Research Service, National Center for Agricultural Utilization Research,
New Crops and Processing Technology Research Unit, 1815 N. University St., Peoria, IL 61604, USA

Received 18 July 2001; received in revised form 9 November 2001; accepted 12 November 2001

Abstract

The direct electrochemical reduction of hemin, protoporphyrin(IX) iron(III) chloride, ligated with strong or weak heterocyclic bases, was investigated in the ionic liquids (IL), 1-butyl-3-methylimidazolium hexafluorophosphate ([bmim][PF₆]) and 1-octyl-3-methylimidazolium hexafluorophosphate ([omim][PF₆]), using cyclic voltammetry and chronocoulometry. Hemin complexed with *N*-methylimidazole (NMI) or with pyridine had $E_{1/2}$ values slightly (4–59 mV) more positive in IL (without electrolyte) than in methanol (1.0 M electrolyte) using a gold electrode. NMI-ligated hemin had a lower $E_{1/2}$ than pyridine-ligated hemin in either IL, consistent with the stronger electron donor characteristic of NMI. [Bmim][PF₆] solutions consistently yielded $E_{1/2}$ values 30 mV more negative than [omim][PF₆] solutions. The diffusion coefficients D_o of hemin in the IL ranged between 1.50 and 2.80×10^{-7} cm² s⁻¹, while the heterogeneous electron-transfer rate constants k_s ranged between 3.7 and 14.3×10^{-3} cm s⁻¹. Cyclic voltammetry of hemin adsorbed to a gold surface through 4,4'-bispyridyl disulfide (AT4) linkages showed a large positive shift in the oxidation wave, indicating that adsorption stabilizes the reduced hemin state. The surface concentration Γ_o of the adsorbed hemin was determined to be 1.21×10^{-10} mol cm⁻², indicating the presence of one or more complete monolayers of hemin. These findings suggest that while hemin is electrochemically active in IL, its behavior is modified by the ligand field strength and surface adsorption phenomena. Published by Elsevier Science B.V.

Keywords: Chronocoulometry; Cyclic voltammetry; Diffusion coefficients; Ionic liquids; Protoporphyrin(IX) iron(III) chloride; Self-assembled monolayers

1. Introduction

There has been increased interest in the development of enzyme-coupled electrodes, especially for use as biosensors, which are active through the enzyme's substrate or through a redox mediator. [1–4]. A more recent development involves the direct electron transfer from the electrode to the enzyme using enzyme-modified electrodes [5–7]. In this case, the enzyme can be adsorbed to the electrode surface, [8,9] encased in a

membrane at the electrode surface, [10] or covalently bound through a surface modifier to the electrode surface [5,11]. The majority of the research involving enzyme-coupled electrodes has been limited to studying their redox activity in buffered aqueous solutions. Although, there has been extensive research into the use of enzymes in non-aqueous media, [12,13] the study of redox active enzymes in non-aqueous media has been limited [14–16].

One class of non-aqueous solvents that may be highly suitable for the study of redox active enzymes is ionic liquids (IL). IL have gained much attention as solvents that hold great promise for green chemistry applications [17–19]. The PF₆⁻ based IL have been shown to be electrochemically stable with a window of over 5 V [20,21]. In addition, IL have been shown to be suitable media for supporting biocatalytic processing [22–25]. The combination of the two technologies leads to the

* Corresponding author. Tel.: +1-309-681-6321; fax: +1-309-681-6524.

E-mail address: compton@ncaur.usda.gov (D.L. Compton).

¹ Product names are necessary to report factually on available data; however, the USDA neither guarantees nor warrants the standard of the product, and the use of the name by the USDA implies no approval of the product to the exclusion of others that may be suitable.

possibility of performing biocatalytic transformations via electrolysis of substrates using enzyme-modified electrodes in IL.

For such a synthetic strategy to be plausible, the enzyme must be electrochemically active in IL. As a first step into investigating the use of enzymatically-modified electrodes in IL, we have examined the electrochemical response of hemin, the simplest biomimetic equivalent to a heme-containing protein, dissolved in IL or adsorbed to a gold electrode immersed in IL. The redox potential of the heme group in hemoproteins is modified by the hydrophobicity of the heme pocket and by the presence of ligands in the iron coordination sphere. In the present work, we test the hypothesis that hemin will undergo quasi-reversible reduction in IL, without added electrolyte, and that hemin redox behavior will be sensitive to the hydrophobicity of the IL and the coordination strength of the ligand.

2. Experimental

2.1. Materials

Hemin (protoporphyrin IX iron (III) chloride, ICN Biomedicals Inc., Aurora, OH) was stored at $-4\text{ }^{\circ}\text{C}$ and used without further purification. Anhydrous *N*-methylimidazole (NMI), pyridine, and MeOH were purchased from Sigma–Aldrich in Sure/Seal™ bottles. Aldrithiol-4 (AT4; 4,4'-bipyridyl disulfide), tetrabutylammonium perchlorate (TBAP), sodium perchlorate, $\text{C}_3\text{H}_6\text{O}$, MeCN, and $\text{C}_6\text{H}_5\text{CH}_3$ were purchased from Sigma–Aldrich and used as obtained (bulk solvents were HPLC grade).

2.2. Ionic liquids

The syntheses of 1-butyl-3-methylimidazolium hexafluorophosphate ([bmim][PF₆]) and 1-octyl-3-methylimidazolium hexafluorophosphate ([omim][PF₆]) have been detailed previously [25]. The purity of the IL was confirmed by ¹H-NMR, and the residual water was determined by Karl–Fischer titration to be $<0.01\%$ (w/w). [25] Elemental analysis performed by Galbraith Laboratories Inc. (Knoxville, TN) showed that the residual Br in the IL was $<0.1\%$. Calc. for [bmim][PF₆](C₈H₁₅N₂PF₆): C, 33.80; H, 5.28; Br, 0.00; F, 40.14; N, 9.86; P, 10.92. Found: C, 33.64; H, 5.59; Br, <0.1 ; F, 36.66; N, 9.76; P, 11.39%. Calc. for [omim][PF₆](C₁₂H₂₃N₂PF₆): C, 42.35; H, 6.76; Br, 0.00; F, 33.53; N, 8.24; P, 9.12. Found: C, 42.15; H, 7.08; Br, <0.1 ; F, 31.89; N, 8.11; P, 9.98%. The relative standard deviations for the elements tested are: C, 0.52; H, 1.33; N, 0.42; P, 4.40; F, 1.26%.

2.3. Cyclic voltammetry

The electrochemical experiments were performed using a BAS CV-50W voltammetric analyzer, a BAS C3 cell stand, Au working electrodes (diameter 1.6 mm), an aq. Ag | AgCl | 3 M NaCl reference electrode (RE), Pt wire auxiliary electrode, and a low volume, water-jacketed CV cell. The entire system was obtained from Bioanalytical Systems (West Lafayette, IN). The water-jacketed cell was heated using a Haake L circulation bath with a Haake D2 temperature controller (Paramus, NJ). All experiments were performed under a dry nitrogen atmosphere, at $40\text{ }^{\circ}\text{C}$, and in triplicate. Data are reported with their standard deviations.

The Au electrodes were cleaned by sonication in pyridine followed by sonication in MeCN and water. Clean electrodes were stored under nitrogen. The electrodes were freshly polished with a 15 μm diamond polish followed by a 1 μm diamond polish (Bioanalytical Systems) before use. The electrodes and nylon polishing pads (Bioanalytical Systems) were rinsed with MeOH and water between polishings.

Naked Au electrodes were used to study solutions of 0.5 mM hemin in 100% molecular solvent (3 ml) and 2.1 mM hemin in 14% (v:v) molecular solvent + IL media (3.5 ml). Experiments performed in 100% MeOH, NMI or pyridine contained 1 M TBAP as an electrolyte. Solutions of hemin in 14% NMI or pyridine + IL were prepared by equilibrating 3 ml of the IL to $40\text{ }^{\circ}\text{C}$ for 15 min in the CV cell then adding 0.5 ml of a 15 mM hemin solution in NMI or pyridine. Blank runs were performed on the IL before the hemin solutions were added.

Hemin-modified Au electrodes were used to study the redox properties of hemin in pure IL. Freshly cleaned and polished Au electrodes were typically treated with 100 mM AT4 + 1 mM hemin solutions in pyridine for 24 h under nitrogen. Excess solution was wicked from the electrode without touching the metal surface, then the electrode was rinsed with IL and used immediately.

2.4. Chronocoulometry

The apparatus described for the cyclic voltammetry (CV) experiments was used for the chronocoulometry experiments performed on the solutions of 0.5 mM hemin in 100% organic media and 2.1 mM hemin in 14% (v:v) molecular solvent + IL media. The potential was stepped towards more negative voltage over a 700 mV window that was centered on the $E_{1/2}$ of each hemin solution determined by CV. All experiments were performed under a dry nitrogen atmosphere, at $40\text{ }^{\circ}\text{C}$, and in triplicate. Data are reported with their relative standard deviations.

The surface areas of three Au electrodes were determined by performing chronocoulometry experiments on

aq. solutions of 2.0 mM $\text{K}_3\text{Fe}(\text{CN})_6$ with 1.0 M KNO_3 as the electrolyte. Based on the diffusion coefficient of aq. $\text{K}_3\text{Fe}(\text{CN})_6$ ($7.6 \times 10^{-6} \text{ cm}^2 \text{ s}^{-1}$), the areas of the Au electrodes were calculated using the Anson equation and the slope of the linear Anson plots (Q vs. $t^{1/2}$) [26]. The determined areas were equivalent to within 1% so subsequent calculations were based on the averaged area, 0.0222 cm^2 .

2.5. Conductivity

Conductivity experiments were performed using a Cole–Parmer (Chicago, IL) conductivity meter (part # 1481-60), a Cole–Parmer Au probe (part # 1481-62, sensitivity $2\text{--}2000 \mu\Omega^{-1} \text{ cm}^{-1}$, 10 cm^{-1} cell constant), and a Cole–Parmer Pt probe (part # 1481-64, sensitivity $2\text{--}200 \text{ m}\Omega^{-1} \text{ cm}^{-1}$, 10 cm^{-1} cell constant). The Pt probe was periodically replatinized using a Cole–Parmer platinizing station and YSI 3140 platinizing solution. The probes were soaked in HPLC grade water 24 h prior to performing the experiments and calibrated versus Oakton standard solutions, 23 through $9000 \mu\Omega^{-1} \text{ cm}^{-1}$ (Cole–Parmer). Measurements were performed at room temperature in 1.5 ml of test solutions in a 1 cm i.d. \times 7.5 cm test tube following the manufacturer's instructions. All measurements were performed in triplicate. The probes were rinsed with MeCN, followed by $\text{C}_3\text{H}_6\text{O}$, and dried with forced air after each experiment.

3. Results and discussion

3.1. Reduction of hemin in ionic liquid solutions

To investigate the electrochemical behavior of hemin in IL, some accommodations to the weak solvating and

high viscosity properties of this medium were made. The direct electrochemical reduction of hemin in solutions of pure [bmim][PF₆] and [omim][PF₆] was limited due to the low solubility of hemin. However, hemin is very soluble in pyridine and NMI (both coordinate to the iron), which when diluted form stable, soluble solutions of hemin in IL. Therefore, the CV of hemin solutions in NMI or pyridine diluted into [bmim][PF₆] and [omim][PF₆] were studied. A minimum of 0.5 mM hemin in the molecular solvent + IL media was required to obtain good signal-to-noise ratios. [Bmim][PF₆] and [omim][PF₆] are viscous solvents at room temperature, 450 and 866 cP, respectively [27]. To facilitate the transfer and mixing of reagents with these IL, all experiments were performed at 40 °C.

Table 1 summarizes the electrochemical data of the CV performed on hemin solutions in molecular solvents and molecular solvent + IL mixtures. All experiments were consistent with a quasi-reversible reduction of hemin (ferric–ferrous redox couple) regardless of the media. Peak separation values (ΔE) were between 62 and 75 mV, while the ratio of cathodic (I_c) and anodic (I_a) peak currents were > 1 . The peak currents for the reduction/oxidation of hemin were linearly dependent on the square root of the scan rate ($r^2 \geq 0.996$) between sweep rates of 50 and 500 mV s^{-1} , as expected for a diffusion-controlled process. It should be noted that, unlike that required for molecular solvents, no supporting electrolyte was required in the IL because of their intrinsic conductivity (see below).

Fig. 1 shows the cyclic voltammograms of hemin + IL media. The mid-point potential values ($E_{1/2}$) of the quasi-reversible reductions of hemin were dependent on both IL and the axial-coordinating ligand used. NMI + IL solutions produced $E_{1/2}$ values up to 216 mV more negative than pyridine + IL solutions. The same trend was true for $E_{1/2}$ values obtained in neat NMI

Table 1
Electrochemical characteristics of ligated hemin in ionic liquids

Solvent	$E_{1/2} \pm \sigma/\text{mV}^d$	$\Delta E \pm \sigma/\text{mV}^d$	$I_c \pm \sigma/\mu\text{A}$	I_c/I_a	$10^7 D_o \pm \sigma/\text{cm}^2 \text{ s}^{-1}$	$10^4 k_s \pm \sigma/\text{cm s}^{-1}$
Pyridine ^a	-52 ± 2	64 ± 2	0.22 ± 0.01	1.28	17.5 ± 2.3	189 ± 19
NMI ^a	-179 ± 1	66 ± 1	0.47 ± 0.03	1.20	18.6 ± 0.3	132 ± 21
Methanol ^a	-176 ± 1	73 ± 1	3.19 ± 0.01	1.30	0.21 ± 0.13	6.53 ± 0.36
Methanol + pyridine ^{a,b}	-99 ± 0	74 ± 1	3.41 ± 0.03	1.16	397 ± 15	263 ± 4
Methanol + NMI ^{a,b}	-330 ± 0	69 ± 0	2.93 ± 0.02	1.12	99.3 ± 1.6	205 ± 1
Methanol + AT4 ^{a,b}	-34 ± 0	75 ± 0	2.81 ± 0.02	1.25	432 ± 7	256 ± 3
Pyridine + [bmim][PF ₆] ^c	-88 ± 3	62 ± 2	0.59 ± 0.02	1.23	2.83 ± 0.20	143 ± 16
Pyridine + [omim][PF ₆] ^c	-55 ± 2	64 ± 2	0.62 ± 0.02	1.18	1.44 ± 0.06	54.0 ± 5.0
NMI + [bmim][PF ₆] ^c	-296 ± 4	68 ± 3	0.58 ± 0.01	1.12	2.54 ± 0.09	37.0 ± 3.0
NMI + [omim][PF ₆] ^c	-271 ± 2	63 ± 4	0.62 ± 0.03	1.23	1.50 ± 0.04	72.0 ± 9.0

σ , Standard deviation.

^a 0.5 mM hemin solutions with 1 M TBAP as the electrolyte.

^b 100 mM pyridine, NMI, or AT4 added to the methanol solution.

^c 2.1 mM hemin solutions in 14% (v:v) pyridine or NMI in the ionic liquid.

^d Potentials reported versus aqueous Ag|AgCl RE at 50 mV s^{-1} and 40 °C.

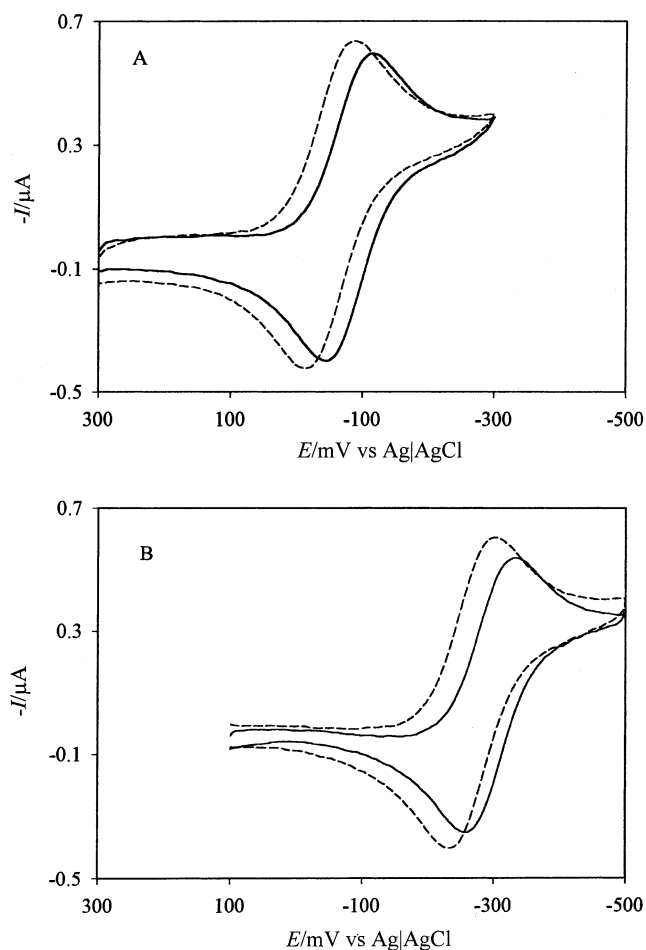


Fig. 1. Cyclic voltammograms of 2.1 mM hemin solutions in: (A) 14% (v/v) pyridine in [bmim][PF₆] (—) and [omim][PF₆] (---); and (B) 14% (v/v) NMI in [bmim][PF₆] (—) and [omim][PF₆] (---). The CV was performed at 50 mV s⁻¹ and 40 °C versus Ag|AgCl. The voltammograms were background subtracted and IR compensated.

and pyridine solutions (Table 1). This effect is attributed to the stronger basicity of NMI (pK_b 6.75) versus pyridine (pK_b 8.63), which allows for better electron donation. The greater electron density near the Fe(III) center presumably makes the hemin more difficult to reduce. Similar effects have been observed with ferrocene substituents in the ionic liquids ethylammonium nitrate and propylammonium nitrate [28]. The redox potential of hemin determined in neat pyridine was slightly (~ 25 mV, correcting for different REs used) more negative than that reported in the literature [29]. This difference is attributed to the higher temperature and higher TBAP concentration used in our experiments.

To study the effect of the axial ligand's basicity on $E_{1/2}$ values better, the influence of IL was eliminated by recording the cyclic voltammograms of 0.5 mM hemin solutions in methanol containing 100 mM NMI, pyridine, or AT4 (Table 1). As expected, when NMI was used as the axial ligand the $E_{1/2}$ values were shifted 154

mV more negative than values obtained in neat methanol. When pyridine was used as the axial ligand, the hemin was 77 mV more easily reduced ($E_{1/2}$ shifted positively) than when in neat methanol. Whereas, NMI acts as a better electron donor, the π -system of pyridine is more electron withdrawing. Therefore, when pyridine is used as the axial ligand, the Fe(III) center of the hemin is more easily reduced. These findings are in agreement with those of Kadish and Bottomley where the $E_{1/2}$ for the reduction of (tetraphenylporphyrin)Fe(III) became more negative upon decreasing the pK_b value of the nitrogenous, axial ligand [30]. Based on its structural similarity to pyridine, AT4 was expected to produce $E_{1/2}$ values near -99 mV in methanol. However, hemin was 65 mV more easily reduced with AT4 as the axial ligand compared to pyridine. The explanation for why AT4, which presumably possesses greater electron donor capabilities than pyridine because of its electron rich disulfide group, results in more positive $E_{1/2}$ potentials is not immediately clear. The trend of more positive $E_{1/2}$ values of ligated hemin, AT4 > pyridine > NMI, was the same in dichloromethane (1.0 M TBAP) solutions (data not shown). Spectroscopically, AT4 was shown to effect the Soret band of 15.3 μ M hemin solutions in methanol similarly compared to pyridine. The Soret band of hemin in methanol (λ_{max} 397 nm) was red shifted upon the addition of 100 mM pyridine (λ_{max} 399 nm) or AT4 (λ_{max} 400 nm). This is less of a red shift than was obtained upon the addition 100 mM NMI (λ_{max} 409 nm) to the hemin solutions in methanol. The spectroscopic data confirm that NMI is a stronger electron donor than the weaker bases and that pyridine and AT4 have a similar effect, therefore similar basicity, on the Fe(III) center. A somewhat more pronounced shift of the hemin Soret band was observed with these ligands in IL, but the trend was preserved: NMI > pyridine = AT4 (data not shown). These findings indicate that PF₆⁻ does not coordinate strongly with the hemin metal center in IL, nor interfere with the coordinating ability of nitrogenous bases.

Differences in the IL cation affected the redox potentials of hemin. When combined with pyridine or NMI, [bmim][PF₆] presents hemin $E_{1/2}$ values ~ 30 mV more negative than [omim][PF₆] (Table 1). The difference in the hemin redox potential between the two IL can be attributed to the variations in the solvent strength and the dielectric constant of the media. [bmim][PF₆] has a slightly higher dielectric than [omim][PF₆] [31,32] and results in more negative redox potentials. The effect of increasing dielectric constant of the medium on the redox potential of hemin is consistent with what has been observed in pyridine (25 °C) solutions containing TBAP, 1.0 M TBAP produced redox potentials 50 mV more negative than solutions containing 0.1 M TBAP. [29]. Note, however, that adding TBAP to IL did not

change hemin $E_{1/2}$ values, reflecting the novel environment afforded by IL. It is clear from these findings that the redox properties of hemin can be modified, not only by the nature of the coordinating ligand but also by the physical properties of the IL.

Nature has evolved a host of heme-centered proteins possessing a wide range of redox potentials attuned to specific functions. The redox potentials of hemoproteins often vary as a result of the different hydrophobicity, polarity, and ligand fields associated with the heme pocket, an effect of varying amino acid side-chains. The use of non-aqueous media can also affect the redox potential of hemoproteins by altering the microenvironment of the heme pocket. Evidence suggests that the redox potentials of some hemoproteins in mixed organic–aqueous media are more dependent on the internal dielectric constant of the protein than the choice of axial ligand [14]. Our findings indicate that for hemin the choice of axial ligand greatly affects the redox potential in IL, which ranges between -55 and -271 mV. The dielectric constant of the IL also effects the hemin redox potential; however, its influence was not as great since the dielectric constants of the two IL were similar. Our studies show that hemin could serve as a biomimetic substitute for hemoproteins in IL with adjustable redox potentials that can be tuned to specific catalytic functions.

3.2. Diffusion coefficients and heterogeneous electron-transfer rates of hemin in ionic liquids

The average diffusion coefficient (D_o) of hemin was determined using the Anson equation [26] and the slope of the linear Anson plots (Q vs. $t^{1/2}$) obtained by chronocoulometry at 40°C (Table 1). The diffusion coefficient of hemin was lower in [omim][PF₆], which is more viscous than [bmim][PF₆]. A similar viscosity dependence was reported for the diffusion of cytochrome *c* through mixed organic–aqueous media [14]. The coordinating ligand did not greatly effect the D_o values of hemin in the IL. The observed diffusion coefficients of ligated hemin in IL were similar to those found for ferrocene [28] and uncomplexed metal cations [33] in ethyl ammonium nitrate. The heterogeneous electron-transfer rate constant (k_s) was determined for hemin in each solvent system (Table 1). Calculations were based on the Nicholson method [34] using the experimentally determined diffusion coefficients and ΔE at 50 mV s^{-1} , assuming $n = 1$, $\alpha = 0.5$, and $T = 40^\circ\text{C}$. Values for ΔE varied up to 10 mV over a 50 to 500 mV scan rate range, indicating that uncompensated potential (*IR*) drop was not present [35]. The k_s values for hemin determined in IL ranged from 10^{-2} to 10^{-3} cm s^{-1} . The pyridine-ligated hemin produced the highest value in [bmim][PF₆], $1.43 \times 10^{-2}\text{ cm s}^{-1}$. The rate constants obtained for hemin in the IL solutions were

comparable to the electron-transfer rates of other Fe(III)–Fe(II) porphyrins in other non-aqueous media. (Tetraphenylporphyrin)FeCl, (octylethylporphyrin)FeCl, (deuteroporphyrin)FeCl, (ethioporphyrin)FeCl, and (protoporphyrin IX)FeCl produced k_s values in *N,N*-dimethylformamide (DMF) between 0.9×10^{-3} and $4.0 \times 10^{-3}\text{ cm s}^{-1}$ [36]. The values for similar porphyrins in dimethyl sulfoxide (DMSO) were closer to 10^{-2} cm s^{-1} [37]. With the exception of pyridine-ligated hemin in [bmim][PF₆], the IL at 40°C produced rate constants closest to those found in DMF at ambient temperatures.

The choice of axial ligand had a greater effect on the electron-transfer rate constant of hemin in [bmim][PF₆] than in [omim][PF₆] (Table 1). In [bmim][PF₆], NMI-ligated hemin produced k_s values fourfold lower than values obtained with pyridine. In contrast, NMI raised the electron-transfer rate of hemin in [omim][PF₆] slightly compared to pyridine-ligated hemin. Contrasting trends of increasing or decreasing electron-transfer rates of ligated hemin by increasing the basicity of the ligand have been previously reported. The rate constant for the Fe(III)–Fe(II) couple of hemin in *N,N'*-dimethylacetamide and DMSO increased with the basicity of the ligating nitrogenous base [37]. However, the rate constant for the reduction of hemin in DMF decreased with increasing $\text{p}K_b$ of the nitrogenous base [36]. The difference between the two trends was attributed to the axial ligand being loosened upon the reduction of hemin in DMF, leading to slower rates. This would suggest that NMI dissociates more readily from hemin in [bmim][PF₆] than in [omim][PF₆] upon reduction. Once the ligand has dissociated, [bmim][PF₆] may better stabilize the hemin in the reduced state. This is corroborated by the larger ΔE value obtained for NMI-ligated hemin in [bmim][PF₆] versus [omim][PF₆], which is the result of a more difficult reoxidation of the iron center.

3.3. Hemin-modified electrodes in ionic liquids

Hemin-modified gold electrodes were prepared to investigate the redox behavior of hemin in neat IL. IL have proven to be good media for electrochemical studies, possessing large potential windows and intrinsic conductivities [20,38]. The conductivities of the IL and solutions of IL used in this study are reported in Table 2. The conductivity of [bmim][PF₆] has been reported previously ($k\ 1460\ \mu\text{S cm}^{-1}$), [20] and our measurements are in agreement, which validates our method. The conductivity of [bmim][PF₆] is fivefold higher than that of [omim][PF₆]. The higher conductivity is attributed to the lower viscosity of [bmim][PF₆]. In the previous experiments (Section 3.1), the conductivity of the IL was increased by dilution with the ligand (Table 2), which decreased the viscosity. The addition of

Table 2
Specific conductance of ionic liquid solutions at 25 °C

Solvent	Solute	$k \pm \sigma / \mu\text{S cm}^{-1}$
[bmim][PF ₆]	None	1440 ± 20
[bmim][PF ₆]	0.1 M <i>n</i> -Bu ₄ ClO ₄	1230 ± 20
[bmim][PF ₆]	14% pyridine	4600 ± 50
[bmim][PF ₆]	14% NMI	3400 ± 50
[omim][PF ₆]	None	259 ± 10
[omim][PF ₆]	0.1 M <i>n</i> -Bu ₄ ClO ₄	213 ± 3
[omim][PF ₆]	14% pyridine	1780 ± 50
[omim][PF ₆]	14% NMI	1240 ± 20

σ , Standard deviation.

TBAP to the IL as an electrolyte decreases the conductivity of both IL, which is attributed to an increase in viscosity. Therefore, no electrolyte was used in the hemin-modified electrode experiments.

Electrochemical studies were performed in neat IL on electrodes modified by hemin linked to the gold surface through AT4. The modification of electrodes with hemin and hemoproteins through mercapto and disulfide containing linkages has been well documented [7,9]. The gold electrodes were prepared by incubation in hemin + AT4 solutions in pyridine for 24 h. Electrodes treated only with AT4 or hemin were electrochemically inactive. Electrodes incubated in hemin + AT4 solutions in NMI were also electrochemically inactive. NMI is a stronger nucleophile than AT4 (see Section 3 above) and is assumed to coordinate preferentially to the axial positions of the hemin. The hemin is therefore unable to coordinate to the AT4 linking group in the presence of NMI, thus rendering the electrode electrochemically inert. Therefore, coordination of adsorbed hemin through the AT4 promoter was essential.

Fig. 2 shows the cyclic voltammograms of hemin AT4-modified gold electrodes in [bmim][PF₆] and [omim][PF₆] recorded at a sweep rate of 50 mV. Experiments were performed at 40 °C to lower the viscosities of the IL to allow for stirring of the solution prior to the cyclic voltammetric measurement. The lower I_a currents obtained in [omim][PF₆] are attributed its lower conductivity. The cyclic voltammograms of the modified electrodes show a quasi-reversible one-electron transfer with ΔE 140 mV ($E_{1/2}$ 15 mV) [39]. The reduction potential of AT4-bound hemin is similar to that of pyridine-ligated hemin solutions in IL. However, the broad reoxidation peak of the AT4-bound hemin is ~150 mV more positive than the pyridine-ligated hemin reoxidation peak in solution. The AT4-bound hemin is more easily reduced in IL (no electrolyte) than hemin adsorbed onto gold with mercaptoethanol in 1.0 M aqueous ClO₄[−] ($E_{1/2}$ −300 mV) [7] or hemin covalently bound to gold in 0.1 M ClO₄[−] in DMSO ($E_{1/2}$ −245 mV) [11]. However, hemin-modified

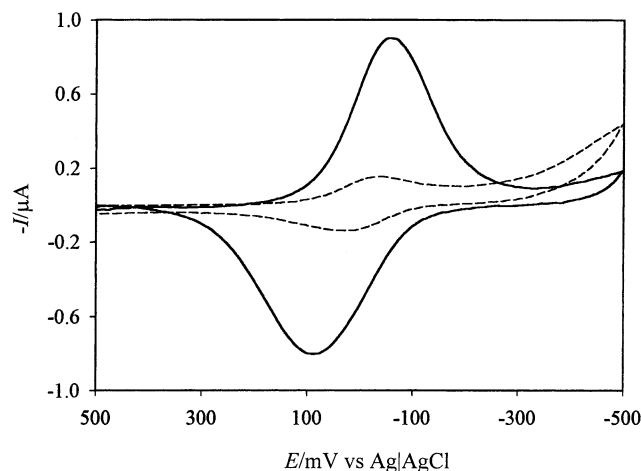


Fig. 2. Cyclic voltammograms of AT4 hemin-modified gold electrodes in [bmim][PF₆] (—) and [omim][PF₆] (---). The CV was performed at 50 mV s^{−1} and 40 °C versus Ag | AgCl. The voltammograms were background subtracted and IR compensated.

gold electrodes undergo slower electron transfer kinetics in IL, as is shown by the larger peak separation, than in electrolytic aqueous or DMSO solutions. The slower electron transfer kinetics may be due to the lower conductivity of the IL, resulting in larger redox peak separation, or effects due to the multilayer adsorption of hemin onto the gold surface (see below). A similar broad peak, large ΔE (~150 mV) cyclic voltammetric response was seen for films of [3Fe-4S] centered *Sulfolobus acidocaldarius* on pyrolytic graphite electrodes in D₂O solutions [40]. The electron transfer of the *S. acidocaldarius* Fe(III)–Fe(II) couple was simple and reversible at low scan rates (1 mV s^{−1}), but showed broadening and separation of the redox peaks at faster scan rates (100 V s^{−1}) due to the inability of the clusters to relax from its more active state during shorter excursions to high potentials. Attempts to run our experiments in IL at slower scan rates failed to produce a measurable voltammetric response.

The surface concentration of hemin adsorbed onto the gold electrodes was determined using chronocoulometry. [41] Anson plots (Q vs. $t^{1/2}$) were obtained for the reduction of the hemin AT4-modified gold electrodes in [bmim][PF₆] at 40 °C over a 700 mV sweep width centered on the $E_{1/2}$, determined by CV. The double layer charging, Q_{dl} , of the electrodes in the IL was measured by two methods: in a separate experiment using an AT4-modified electrode blank and by double potential step chronocoulometry. The surface concentration of hemin, Γ_o , was 3.34×10^{-10} mol cm^{−2} when Q_{dl} was estimated using an AT4-modified electrode in a separate experiment. The more accurate correction of Q_{dl} by double potential step chronocoulometry resulted in a Γ_o of 1.21×10^{-10} mol cm^{−2}. Both values indicate more than a single monolayer of coverage based on the theoretical surface coverage, Γ_o .

6.98×10^{-11} mol cm $^{-2}$, assuming a hemin plane oriented parallel to the surface, the dimensions of a single hemin molecule being $14 \times 17 \times 3$ Å, and an electroactive surface area of 0.0222 cm 2 . Parallel stacking of hemin through AT4 axial linkages could lead to multilayer coverage. Gorton et al. reported a hemin surface concentration of 0.44×10^{-10} mol cm $^{-2}$ on gold electrodes adsorbed through mercaptoethanol linkages [7]. Our studies show that AT4 permits double the surface density of hemin compared to mercaptoethanol, resulting in cyclic voltammograms with more pronounced currents at lower scan rates.

4. Conclusions

Hemin undergoes a quasi-reversible, one-electron reduction in IL solutions. The redox potential of hemin varies as a function of the IL and the coordinating ligand. The more polar [bmim][PF $_6$] produces reduction potentials 30 mV more negative than [omim][PF $_6$], regardless of the coordinating ligand. It is assumed that the hemin Fe(III)–Fe(II) redox couple could be adjusted over a greater potential range using IL with higher or lower polarity. The coordinating ligands, NMI or pyridine, had a greater effect on the hemin redox couple, resulting in a potential range of 245 mV. NMI ligated-hemin produced the most negative redox potentials in IL solutions. The diffusion coefficients of ligated hemin in the IL (D_o , 10^{-7} cm 2 s $^{-1}$) and the heterogeneous electron-transfer rates (k_s , 10^{-3} cm s $^{-1}$) were similarly affected by the choice of IL. The less viscous [bmim][PF $_6$] produced hemin D_o values approximately twofold greater than values obtained in [omim][PF $_6$], regardless of the ligand present. The k_s values, however, were ligand dependent with pyridine-ligated hemin producing slower rates than NMI-ligated hemin in [omim][PF $_6$]. The ligands produced the opposite effect on hemin rate constants in [bmim][PF $_6$].

AT4 hemin-modified gold electrodes were used to study the reduction of hemin in neat IL. The hemin density on the electrode surface was twice (1.21×10^{-10} mol cm $^{-2}$) the density calculated for a theoretical monolayer and threefold greater than the density obtained by Gorton et al. using mercaptoethanol as the linking group [7]. The cyclic voltammograms of hemin-modified gold electrodes showed more pronounced currents in IL without added electrolyte, even at lower scan rates, than hemin-modified gold electrodes in 0.1 M ClO $_4^-$ aqueous or 1.0 M ClO $_4^-$ DMSO solutions. These results suggest that hemin and hemin-modified electrodes have the potential to be used in IL, without electrolyte, as biomimetic equivalents of heme-containing proteins for a variety of bioelectrosyntheses. The reduction potential of the hemin can be adjusted by varying the polarity of the IL or the basicity of the

coordinating ligand. This will allow for the tuning of the hemin redox couple to specific potentials for catalyzing a wide variety of synthetic reactions in the neoteric, ‘green’ IL media.

Acknowledgements

The authors thank Mary M. Hallengren and Leslie J. Smith for their excellent technical assistance.

References

- [1] T. Nakaminami, S.-I. Ito, S. Kuwabata, H. Yoneyama, *Anal. Chem.* 71 (1999) 4278.
- [2] B. Wang, B. Li, Z. Wang, G. Xu, Q. Wang, S. Dong, *Anal. Chem.* 71 (1999) 1935.
- [3] S.A. Kane, I. Iwuoha, M.R. Smyth, *Analyst* 123 (1998) 2001.
- [4] E. Katz, V. Heleg-Shabtai, A. Bardea, I. Willner, H.K. Rau, W. Haehnel, *Biosens. Bioelectron.* 13 (1998) 741.
- [5] C. Ruan, R. Yang, X. Chen, J. Deng, *J. Electroanal. Chem.* 455 (1998) 121.
- [6] A.L. Ghindilis, P. Atanasov, E. Wilkins, *Electroanalysis* 9 (1997) 661.
- [7] L. Gorton, A. Lindgren, T. Larsson, F.D. Munteanu, T. Ruzgas, I. Gazaryan, *Anal. Chim. Acta* 400 (1999) 91.
- [8] H.A.O. Hill, L.H. Guo, in: R.A. Scott, A.G. Mauk (Eds.), *Cytochrome c: A Multidisciplinary Approach*, University Science Books, Sausalito, CA, 1996, pp. 317–333.
- [9] M. Fedurco, *Coord. Chem. Rev.* 209 (2000) 263.
- [10] T. Ferri, A. Poscia, R. Santucci, *Bioelectrochem. Bioenerg.* 44 (1998) 177.
- [11] T. Lötzbeyer, W. Schumann, H.-L. Schmidt, *J. Electroanal. Chem.* 395 (1995) 341.
- [12] A. Koskinen, A.M. Klivanov (Eds.), *Enzymatic Reactions in Organic Media*, Chapman & Hall, London, 1996.
- [13] M.N. Gupta, *Eur. J. Biochem.* 203 (1992) 25.
- [14] S. Sivakolundu, P.A. Mabrouk, *J. Am. Chem. Soc.* 122 (2000) 1513.
- [15] P.A. Mabrouk, T.G. Spiro, *J. Am. Chem. Soc.* 120 (1998) 10303.
- [16] P.A. Mabrouk, *Anal. Chem.* 68 (1996) 189.
- [17] J.G. Huddleston, H.D. Willauer, R.P. Swatloski, A.E. Visser, R.D. Rogers, *Chem. Commun.* (1998) 1765.
- [18] K.R. Seddon, *J. Chem. Technol. Biotechnol.* 68 (1997) 351.
- [19] V.R. Koch, C. Nanjundiah, R.T. Carlin, US Patent 5,827,602, 1998.
- [20] R. Hagiwara, Y. Ito, *J. Fluorine Chem.* 105 (2000) 221.
- [21] P. Bonhote, A.-P. Dias, US Patent 5,683,832, 1997.
- [22] S.G. Cull, J.D. Holbrey, V. Vargas-Mora, K.R. Seddon, G.J. Lye, *Biotechnol. Bioeng.* 69 (2000) 227.
- [23] M. Erbeldinger, A.J. Mesiano, A.J. Russel, *Biotechnol. Prog.* 16 (2000) 1129.
- [24] R. Madeira Lau, F. van Rantwijk, K.R. Seddon, R.A. Sheldon, *Org. Lett.* 2 (2000) 4189.
- [25] J.A. Laszlo, D.L. Compton, *Biotechnol. Bioeng.* 75 (2001) 181.
- [26] F.C. Anson, *Anal. Chem.* 38 (1966) 54.
- [27] J.G. Huddleston, A.E. Visser, W.M. Reichert, H.D. Willauer, G.A. Broker, R.D. Rogers, *Green Chem.* 3 (2001) 156.
- [28] J.B. Shotwell, R.A. Flowers II, *Electroanalysis* 12 (2000) 223.
- [29] K.M. Kadish, K.M. Smith, R. Guilard (Eds.), *The Porphyrin Handbook*, vol. 9, Academic Press, San Diego, 2000, pp. 188–189.
- [30] K.M. Kadish, L.A. Bottomley, *Inorg. Chem.* 19 (1980) 832.

- [31] S.N.V.K. Aki, J.F. Brennecke, A. Chem. Comm. (2001) 413.
- [32] M.J. Muldoon, C.M. Gordon, I.R. Dunkin, J. Chem. Soc. Perkin Trans. 2 (2001) 433.
- [33] H. Schnider, J. Stroka, Polish J. Chem. 68 (1994) 795.
- [34] R.S. Nicholson, Anal. Chem. 37 (1965) 1351.
- [35] F.M. Hawkrige, I. Taniguchi, in: K.M. Kadish, K.M. Smith, R. Guillard (Eds.), The Porphyrin Handbook, vol. 8, Academic Press, San Diego, 2000, pp. 191–202.
- [36] K.M. Kadish, G. Larson, Bioinorg. Chem. 7 (1977) 95.
- [37] L.A. Constant, D.G. Davis, J. Electroanal. Chem. 74 (1976) 85.
- [38] J. Fuller, A.C. Breda, R.T. Carlin, J. Electrochem. Soc. 144 (1997) L69.
- [39] A.J. Bard, L.R. Faulkner (Eds.), Electrochemical Methods, Wiley, New York, 1980, pp. 519–528.
- [40] J. Hirst, G.N.L. Jameson, J.W.A. Allen, F.A. Armstrong, J. Am. Chem. Soc. 120 (1998) 11994.
- [41] W.R. Heineman, Curr. Sep. 7 (1986) 58.